Escola de Ciências

Universidade do Minho

Bachelor degree in Physics

Investigation Project

Dark Solitons and Breathers as solutions of the NonLinear Schrödinger Equation

Author:
Francisco Lobo

Supervisor:
Yuliy Bludov

Braga, 2020/2021

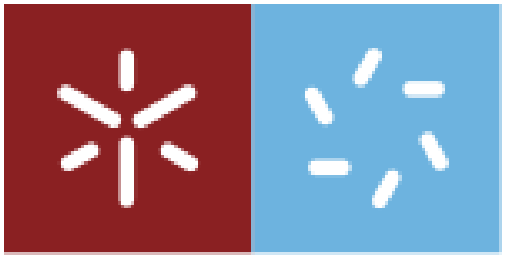

Abstract

This project deals with the nonlinear dynamics of solitons - localized waves that maintain their shape due to balance between its natural diffraction and self-focusing (or self-defocusing) nonlinearity - and the nonlinear dynamics of breathers - strongly localized solitonic structures that oscillate periodically in either space, time or both. Firstly, we modulate the instability of a plane wave background in the presence of small perturbations and show the appearance of two different medium, the focusing medium and the defocusing medium. Secondly, we derive analytically from the NonLinear Schrödinger Equation with cubic nonlinearity in a self-defocusing media the spacial solutions of the dark and gray soliton. For last, we derive analytically, this time in a self-focusing medium, the Akhmediev breather solution and show that by varying the interval of a parameter one can obtain the Kuznetsov-Ma breather and the Peregrine soliton solutions.

Este projeto trata da dinâmica não linear dos solitões - ondas localizadas que mantêm a sua forma devido ao equilíbrio entre a difração natural e a difração não linear - e a dinâmica não linear dos respiradores - estruturas solitónicas fortemente localizadas que oscilam periodicamente no espaço, no tempo ou em ambos. Em primeiro lugar, modulamos a instabilidade de um fundo de onda plana na presença de pequenas perturbações e mostramos o aparecimento de dois diferentes meios, o meio de focagem e o meio de desfocagem. Em segundo lugar, derivamos analiticamente da Equação de Schrödinger Não Linear com não-linearidade cúbica num meio auto-desfocagem as soluções espaciais de solitão cinzento e escuro. Por último, derivamos analiticamente, desta vez num meio de auto-focagem, a solução do respirador de Akhmediev e mostramos que, variando o intervalo de um parâmetro, se pode obter também a solução do respirador de Kuznetsov-Ma e do solitão Peregrine.

Keywords: Nonlinear Schrödinger Equation, Modulation Instability, Soliton, Dark Soliton, Gray Soliton, Breather, Kuznetsov-Ma Breather, Akhmediev Breather, Peregrine Soliton

Contents

1. Introduction

The theory of solitons can be applied to various areas of physics such as optical fibers [1], deep [2] and shallow [3] water dynamics, dynamics of cold atoms in Bose-Einstein condensates [4], electromagnetic waves in dielectrics with Kerr nonlinearity (like graphene [5], waveguides [6], and other similar media). For instance, in the field of optics, the theory of solitons deals with spatial and temporal [7, 8] Kerr soliton solutions but also with many other types of solitons such as spatiotemporal solitons [9] (often called light bullets), Bragg [10] and gap [11] solitons in periodically modulated systems, discrete solitons in waveguide arrays [12] and photonic crystals [13].

As an example, in Kerr optics, solitons can be formed owing to the induced refractive index change [14] of the medium, which is proportional to the **square** of the electric field, or alternatively, proportional to the intensity of the light. In detail, if the initial pulse has a certain profile and high enough intensity, the changes on the refractive index can be such that the pulse becomes self-trapped by its self-induced optical fiber waveguide. On one hand, natural/linear dispersion arises because the velocity of the pulse depends on its wavelength (bigger wavelengths travel faster than smaller wavelengths) but, on the other hand, the Kerr/nonlinear dispersion arises because the velocity of the pulse depends on its amplitude (bigger amplitudes travel faster than smaller amplitude) causing the pulse to steepen like a sea wave [15]. Because one can show that for soliton waves bigger wavelengths have smaller amplitudes, when both linear and nonlinear effects are present, the increment in velocity caused by the linear dispersion cancels out with the decrement in velocity caused by the nonlinear dispersion such that the pulse stay stable. This leads to the formation of a spatial solitons, a pulse that propagates maintaining its shape and velocity [16].

In this work we derive analytically dark [17] and gray [18] solitons, a family of solutions in a defocusing medium which appears as moving dips within a constant amplitude background travelling with a velocity dependent on the amplitude. The term "dark" originated from nonlinear optics since this type of solution appears as localized light intensity dips i.e., dark dots in an otherwise bright background. The term "gray" relates to the similar solutions with dimmer light intensity dips [19]. Dark solitons are of special interest because its solution is stationary, its intensity profile goes to zero at the soliton's center and its phase profile has an abrupt phase shift of π also at the soliton's center [20].

For context, we briefly discuss and compare another soliton solution. In contrast with dark solitons, bright solitons [21] appear as moving bright dots in an otherwise dark background. Contrarily to dark solitons, they form in a focusing medium within a null background with a boundary condition on the amplitude function to vanish as $|x| \to \infty$ [22]. Another interesting difference is that a bright soliton has a constant phase opposed to the chirping nature of the dark soliton, as we will see in the next section.

Along with the already mentioned solutions (which are characterized by the fact that they propagate without losing the shape of its squared amplitude), the NLSE possesses another kind of solutions known as breathers [23]. These solutions are non-stationary and its squared amplitudes exhibits localized periodical oscillations. We derive analytically a family of three of this breather solutions, the Kuznetsov-Ma breather [24, 25], the Akhmediev breather [26, 27] and the Peregrine soliton [28]. This solutions are very similar and can be obtained from one another by varying a parameter in a certain range. The term "breather" alludes to the characteristic that most of this solutions are localized in space and oscillate in time (like a snorkeller swimming up gasping for air), as is the case for the Kuznetsov-Ma breather [29]. Actually, the term "breather" can also refer to solutions that are localized in time and oscillate in space, as is the case of the Ahkmediev breather, or solutions that are localized both in time and space, as is the case of the Peregrine soliton [30].

Among the breathers, the Peregrine soliton is of special interest because it resembles "rogue waves", giant waves that appear from nowhere and disappear without a trace [31]. The "rogue wave" concept is embedded in nearly all areas of physics and has a wide range of applications due to its property of being localized in both time and space. They can serve as a model of elementary particles, make certain periodic patterns that resemble atomic like structures [32], etc...

2. Modulational Instability

In this section we consider the simplest solution of the (1+1)D Nonlinear Schrödinger Equation (NLSE) in the form of a plane wave and show that under certain conditions it can be either stable or unstable with respect to small perturbations. This phenomenon is known as *modulational instability*.

The nonlinear Schrödinger equation, written for the dimensionless time t, coordinate x and nonlinearity σ

$$i\frac{\partial\psi}{\partial t}+\frac{\partial^2\psi}{\partial x^2}+\sigma|\psi(x,t)|^2\psi(x,t)=0, \tag{1}$$

admits the simplest solution in the form of a plane wave

$$\psi(x,t)=\rho\exp(iQx-i\Omega t). \tag{2}$$

Here ρ is the amplitude, Q and Ω are the wave number and angular frequency, respectively. Substituting Eq.(2) into Eq.(1) we obtain the dispersion relation

$$\Omega=Q^2\pm\sigma\rho^2. \tag{3}$$

Thus, a plane wave that propagates through a nonlinear medium acquires a phase shift dependent on its amplitude squared ρ^2. Note that, in a linear medium (where $\sigma=0$) the phase shift does no longer depends on ρ^2 as intended.

In the case of an homogeneous solution, which is of special interest, the dependency on the propagation distance x no longer exists ($\partial/\partial x=0$) and so, the solution and its respective dispersion relation reduces to

$$\psi(x,t)=\rho\exp\big(i\sigma\rho^2t\big),\quad \Omega=-\sigma\rho^2. \tag{4}$$

Now a natural question appears: how stable is the obtained solution with respect to small perturbations? To answer this question we represent a perturbation as a superposition of two propagating waves in opposite directions, $V(x,t)=A\exp(iqx-i\omega t)+B^*\exp(-iqx+i\omega^*t)$, with amplitudes much smaller than that of the plane wave background, this is $|V(x,t)|\ll\rho$. The perturbed solution will have the form

$$\psi(x,t)=[\rho+V(x,t)]\exp\big(i\sigma\rho^2t\big). \tag{5}$$

Substituting the perturbed solution back into Eq.(1) and leaving only the linear terms of the perturbation $V(x,t)$, we obtain

$$i\frac{\partial V}{\partial t} + \frac{\partial^2 V}{\partial x^2} + \sigma\rho^2\left[V(x,t) + V^*(x,t)\right] = 0. \tag{6}$$

If we expand the potential,

$$\begin{aligned} &\omega A\exp(iqx - i\omega t) - \omega^* B^*\exp\left(-iqx + i\omega^* t\right) - \\ &-q^2\left[A\exp(iqx - i\omega t) + B^*\exp\left(-iqx + i\omega^* t\right)\right] + \\ &+\sigma\rho^2\Big[A\exp(iqx - i\omega t) + B^*\exp\left(-iqx + i\omega^* t\right) + \\ &+ A^*\exp\left(-iqx + i\omega^* t\right) + B\exp(iqx - i\omega t)\Big] = 0, \end{aligned} \tag{7}$$

and collect the terms of each exponential, we obtain the system of coupled linear equations

$$\begin{cases} \left[\omega - q^2 + \sigma\rho^2\right]A + \sigma\rho^2 B = 0, \\ \sigma\rho^2 A + \left[-\omega - q^2 + \sigma\rho^2\right]B = 0. \end{cases} \tag{8}$$

The dispersion relation is obtained by matching the linear system's determinant to zero,

$$\omega = \pm|q|\sqrt{(q^2 - 2\sigma\rho^2)}. \tag{9}$$

From this expression its possible to distinguish two distinct cases.

On one hand, if $\sigma < 0$ (*self-defocusing* case), the frequency of the perturbation ω is a purely real value and so, the perturbation $V(x,t)$ will be oscillating in time and will not grow, leading to a stable, constant-intensity plane wave background.

On the other hand, if $\sigma > 0$ (*self-focusing* case), the instability of the plane wave is determined by the value of q. If $q > \sqrt{2\sigma}\rho$ we have a real value under the root and so, the frequency ω will be a purely real value and the plane wave solution stays stable. But, if $q < \sqrt{2\sigma}\rho$, the value under the square root becomes negative, the frequency ω becomes a purely imaginary value, and now the perturbation $V(x,t)$ grows exponentially in time. The plane wave background will grow in an unstable manner, and eventually will deviate from the initial profile.

To see how the instability grows for different perturbations we introduce the *modulational instability gain* as $g(q) = |\,\mathrm{Im}(\omega(q))|$, where bigger values of $g(q)$ indicate more rapidly growing instability. In Fig.1 we plotted the instability gain $g(q)$ as a function of the perturbation's wave number q for several values of the initial amplitude of the plane wave ρ with $\sigma = 1$. The maximum instability occurs at $q = \rho$ with values of maximum gain $g_{max} = \rho^2$.

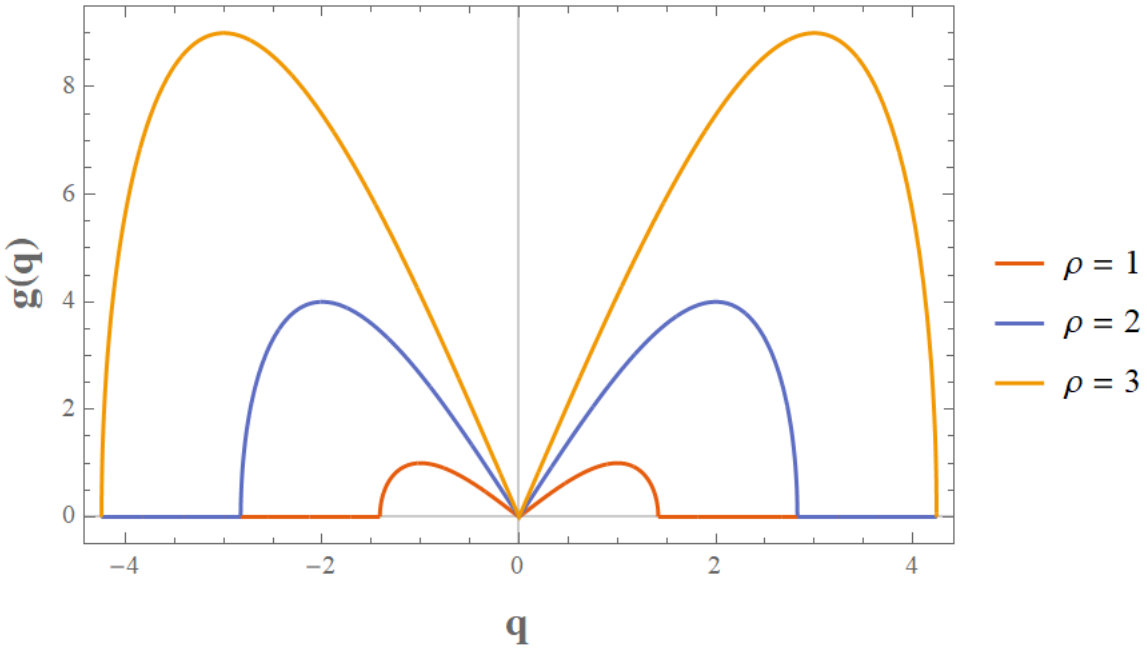

Figure 1: Modulation-instability gain $g(q)$ as a function of the perturbation's wave number q for several values of the initial amplitude of the plane wave $\rho = 1, 2, 3$ with $\sigma = 1$.

3. Dark Soliton

3.1. Dark Soliton

A dark soliton is a shape-preserving solution which appears as a stationary dip in a constant amplitude background. To find its solution, we can start by making an educated guess that its profile function $\phi(x)$ needs to be real and independent of time, this way the solution will maintain its shape at all times. We can always introduce a phase that, in the case of an homogeneous solution, depends only on time. The inicial ansatz is

$$\psi(x,t) = \phi(x)e^{-i\Omega t}. \tag{10}$$

Dark solitons can be formed only on a stable plane wave background of constant amplitude ρ. From the modulational instability analysis (performed in Sec.2) we already found that stable backgrounds take place in a self-defocusing medium ($\sigma < 0$). We consider $\sigma = -1$ and rewrite the NLSE as

$$i\frac{\partial\psi}{\partial t} + \frac{\partial^2\psi}{\partial x^2} - |\psi(x,t)|^2\psi(x,t) = 0. \tag{11}$$

Given the constant amplitude background, we impose the boundary conditions to be

$$\phi(0,x) = \begin{cases} \pm\rho & , \text{ for } x \to -\infty. \\ \mp\rho & , \text{ for } x \to +\infty. \end{cases} \tag{12}$$

Substituting the ansatz in Eq.(10) in the NLSE in Eq.(11) we obtain

$$\Omega\phi + \phi_{xx} - \phi^3 = 0. \tag{13}$$

Note that, because the profile function $\phi(x)$ is real, the last term is just $\phi^3(x)$. We multiply both sides by $2\phi_x$ and rewrite it as

$$\Omega\frac{d\phi^2}{dx} + \frac{d}{dx}\left(\frac{d\phi}{dx}\right)^2 - \frac{1}{2}\frac{d\phi^4}{dx} = 0. \tag{14}$$

Integrating both sides with respect to x we then have

$$\Omega\phi^2 + (\phi_x)^2 - \frac{1}{2}\phi^4 = C, \tag{15}$$

with C being the integration constant.

The boundary conditions in Eq.(12) and the dip nature of a dark soliton tells us that the solution asymptotically approaches the constant background amplitude and thus its derivative will eventually go to zero. Under this condition, the constant C takes the value

$$C = \Omega\rho^2 - \frac{1}{2}\rho^4 = \frac{\Omega^2}{2}. \tag{16}$$

Substituting Eq.(16) back in Eq.(15) we obtain the differential equation

$$\phi_x = \pm\sqrt{\frac{\Omega^2}{2} - \Omega\phi^2 + \frac{1}{2}\phi^4} = \pm\frac{1}{\sqrt{2}}(\Omega - \phi^2). \tag{17}$$

This is easily solvable by isolating the ϕ terms in one side

$$\frac{d\phi}{\Omega - \phi^2} = \pm\sqrt{\frac{1}{2}}dx \tag{18}$$

and then integrating both sides making the substitution $y = \sqrt{1/\Omega}\ \phi(x)$

$$\int \frac{dy}{1 - y^2} = \pm\sqrt{\frac{\Omega}{2}}\int dx. \tag{19}$$

The integral on the left-hand side gives $arctanh(y)$, hence the solution for our profile function is

$$\phi(x) = \pm\sqrt{\Omega}\tanh\left[\sqrt{\frac{\Omega}{2}}(x - x_0)\right], \tag{20}$$

with x_0 being the soliton's dip center. Substituting $\phi(x)$ back in Eq.(10) we obtain the general solution for a stationary dark solution

$$\psi_D(x,t) = \pm\sqrt{\Omega}\tanh\left[\sqrt{\frac{\Omega}{2}}(x - x_0)\right]e^{-i\Omega t}, \tag{21}$$

where $\Omega > 0$. It has a squared modulus of

$$|\psi_D(x,t)|^2 = \Omega\tanh^2\left[\sqrt{\frac{\Omega}{2}}(x - x_0)\right]. \tag{22}$$

We plotted $|\psi_D(x,t)|^2$ in Fig.3(b) as a function of time and propagation distance x. Because $|\psi_D(x,t)|^2$ does not depend on time this solution is stationary. In Fig.2(a) we plotted various profile's of the solution $\psi_D(x)$ and in Fig.2(b) its squared modulus $|\psi_D(x,t)|^2$ for different values of Ω at $t = 0$. Notice that the amplitude goes to zero at the soliton's dip center - a principal characteristic of all dark solitons.

Owing to the antisymmetric nature of the *tanh* function, the soliton's phase undergoes an abrupt π shift at the dip center as shown in Fig.2(c), namely

$$Arg(\psi_D(x,t)) = \begin{cases} \pi - \Omega t & , \text{ for } x < 0, \\ -\Omega t & , \text{ for } x > 0. \end{cases} \tag{23}$$

Among other characteristics of the dark soliton, the dependence of its width on the background amplitude $\rho = \sqrt{\Omega}$ is of great interest. This dependence is depicted in Fig.2(d). We rewrite the soliton solution as

$$\psi_D(x) = \sqrt{\Omega}\tanh(x/L), \tag{24}$$

with $L = \sqrt{2/\Omega}$ being the dark soliton width. Higher amplitudes of the background $\rho = \sqrt{\Omega}$ correspond to the lower widths of the dark soliton, supported by this background.

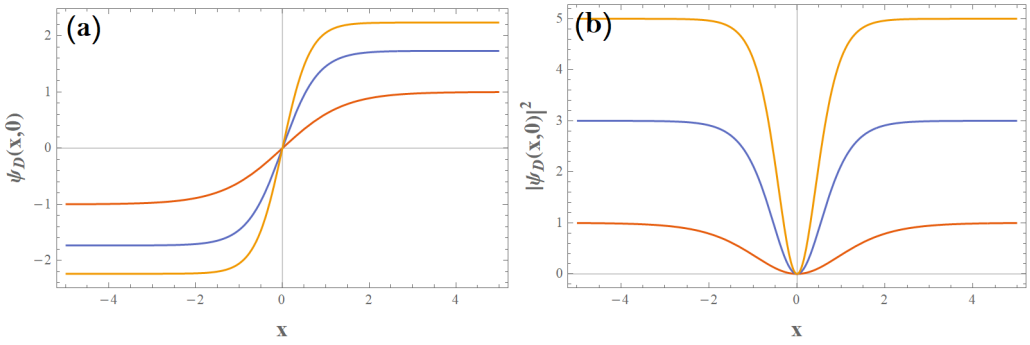

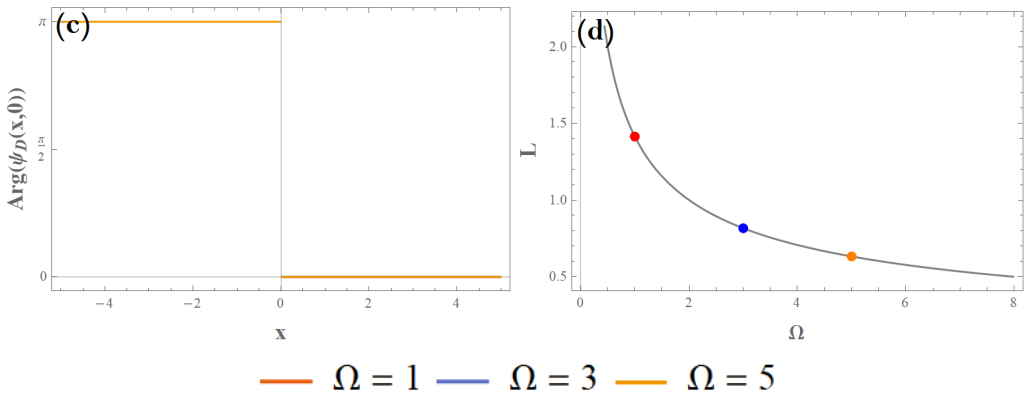

Figure 2: Profiles at $t = 0$ for various values of Ω (depicted in the legend) of **(a)** dark soliton solutions $\psi(x, 0)$, **(b)** its magnitudes squared $|\psi(x, 0)|^2$ and **(c)** its phases $Arg(\psi(x, 0))$. The phase profiles at t=0 coincide for all Ω. In **(d)** we represent the dependence of the dark soliton width L on the frequency Ω [frequencies of solitons in **(a)**–**(c)** are depicted by the dots of respective colors in **(d)**].

3.2. Gray Soliton

Gray solitons are in the same family of solutions as the dark solitons, they both are shape-preserving solutions which appear as dips in a constant amplitude background. They differentiate from each other because the gray soliton solution is not stationary - it propagate with constant velocity, which depends on the background amplitude. In addition, a gray soliton has a non-zero intensity profile at the dip's center and do not has the abrupt π phase shift, instead this phase shift is more gradual and smooth along space. As it will be shown, both the intensity at the dip center and the phase-shift are determined by the soliton velocity.

We start by making the educated guess that, if the soliton is non-stationary and is moving with a constant velocity v ,then its solution can be expressed in the form of a travelling wave

$$\psi(x, t) = [f(x - vt) + ig(x - vt)] \exp(-i\Omega t). \tag{25}$$

Here $f(x - vt)$ and $g(x - vt)$ are supposed to be real functions. We introduce the substitution variable $\xi = x - vt$ and right away substitute this anzatz into the NLSE with $\sigma = -1$ in Eq.(11) (as we did for the dark soliton). Note that, because of the change of variable, we have $\partial/\partial x = \partial/\partial\xi$ and $\partial/\partial t = -v\partial/\partial\xi$. After the above-mentioned substitution, we have

$$\Omega[f + ig] - iv[f_\xi + ig_\xi] + [f_{\xi\xi} + ig_{\xi\xi}] - [f^2 + g^2][f + ig] = 0 \tag{26}$$

Separating the real and imaginary part we get the coupled system of two equations

$$\Omega f + v g_\xi + f_{\xi\xi} - [f^2 + g^2] f = 0, \tag{27}$$
$$\Omega g - v f_\xi + g_{\xi\xi} - [f^2 + g^2] g = 0. \tag{28}$$

Multiplying Eq.(27) by $2f_\xi$ and Eq.(28) by $2g_\xi$ and summating results we get

$$2\Omega f f_\xi + 2 f_\xi f_{\xi\xi} + 2\Omega g g_\xi + 2 g_\xi g_{\xi\xi} - 2[f^3 f_\xi + g^2 f f_\xi + f^2 g g_\xi + g^3 g_\xi] = 0. \tag{29}$$

Integrating the above equation, we obtain the first integral

$$\Omega f^2 + (f_\xi)^2 + \Omega g^2 + (g_\xi)^2 - \left[\frac{1}{2} f^4 + f^2 g^2 + \frac{1}{2} g^4\right] = C_1. \tag{30}$$

Here C_1 is the constant of integration, which can be found from the boundary condition. The absolute value of the function at $\xi = \pm\infty$ is $|\psi(\pm\infty, t)| = \rho = \sqrt{\Omega}$ or, in other words, $f(\pm\infty)^2 + g(\pm\infty)^2 = \Omega$. As we did for the dark soliton, since the solution at $\xi = \pm\infty$ asymptotically approaches the plane wave background its derivative approaches zero at $\xi = \pm\infty$. From these two conditions we obtain the constant of integration to be

$$C_1 = \Omega^2/2. \tag{31}$$

To obtain the second integral of Eqs.(27) and (28), we multiply Eq.(27) by $2g$ and Eq.(28) by $2f$ and subtract the resulting equation instead. We get

$$2 v g_\xi g + 2 v f_\xi f + 2 f_{\xi\xi} g - 2 g_{\xi\xi} f = 0, \tag{32}$$

and, if we integrate on both sides we obtain

$$v[f^2 + g^2] + 2 f_\xi g - 2 g_\xi f = C_2, \tag{33}$$

with C_2 being the integration constant. Applying the above-mentioned boundary conditions, we have

$$C_2 = v\Omega. \tag{34}$$

Note that Eq.(30) and Eq.(33) possess an important property: if f and g are solutions then

$$\begin{pmatrix} \widetilde{f} \\ \widetilde{g} \end{pmatrix} = \begin{pmatrix} \cos\varphi & -\sin\varphi \\ \sin\varphi & \cos\varphi \end{pmatrix} \begin{pmatrix} f \\ g \end{pmatrix} \tag{35}$$

are also solutions, which correspond to the adding of a constant phase to the solution in Eq.(25), namely $\widetilde{\psi} = \psi \exp(i\varphi)$.

We seek the solutions of Eq.(30) and Eq.(33) for the case when g does not depend on ξ, this is, $g = G$ is now a constant. In this case Eq.(30) and Eq.(33) can be rewritten in the form

$$f_\xi = \pm\frac{1}{\sqrt{2}}[\Omega - (f^2 + G^2)]. \tag{36}$$

$$f_\xi = \quad \frac{v}{2G}[\Omega - (f^2 + G^2)]. \tag{37}$$

From this expressions we get that $G = \pm v/\sqrt{2}$. We rewrite them as

$$f_\xi = \pm\frac{1}{\sqrt{2}}\left[\Omega - \frac{v^2}{2} - f^2\right] \tag{38}$$

In full analogy with the previous section, we can find the solution of the above equation to be

$$f(x - vt) = \pm\sqrt{\Omega - \frac{v^2}{2}}\tanh\left[\sqrt{\frac{\Omega}{2}\left(1 - \frac{v^2}{2\Omega}\right)}(x - vt - x_0)\right]. \tag{39}$$

As a result, the solution of a gray soliton has the form

$$\psi_G(x,t) = \sqrt{\Omega}e^{-i\Omega t}\left(i\frac{v}{v_c} + \sqrt{1 - \frac{v^2}{v_c^2}}\tanh\left[\sqrt{\left(1 - \frac{v^2}{v_c^2}\right)\frac{\Omega}{2}}(x - vt)\right]\right). \tag{40}$$

where $v_c = \sqrt{2\Omega}$ is the critical velocity such that $v < v_c$ and the dip's center x_0 is chosen to be at $x_0 = 0$.

It's useful to employ a single parameter θ (remember that $\sqrt{\Omega}$ represents the background amplitude, it's not a parameter) by identifying

$$\sin\theta = \frac{v}{v_c} \text{ and } \cos\theta = \sqrt{1 - \frac{v^2}{v_c^2}} \tag{41}$$

Notice that the velocity of the soliton v is dependent on the background amplitude Ω through the parameter θ. In the special case of $\theta = 0$, the velocity v goes to zero and we recover the dark soliton solution in Eq.(21). We rewrite the solution as

$$\psi_G(x,t) = \sqrt{\Omega} e^{-i\Omega t} \left(i\sin(\theta) + \cos(\theta)\tanh\left[\frac{\sqrt{\Omega}}{\sqrt{2}} \cos(\theta)\Big(x - \sqrt{2\Omega}\sin(\theta) t \Big) \right] \right), \tag{42}$$

with a squared modulus of

$$|\psi_G(x,t)|^2 = \Omega \left(\sin^2(\theta) + \cos^2(\theta)\tanh^2\left[\frac{\sqrt{\Omega}}{\sqrt{2}} \cos(\theta)\Big(x - \sqrt{2\Omega}\sin(\theta) t \Big) \right] \right). \tag{43}$$

In Fig.3(a) we plotted $|\psi_G(x,t)|^2$ as a function of time and propagation distance with $\Omega = 1$ and $\theta = 3\pi/16$. As it can be seen, the gray soliton is moving with constant velocity $v = \sqrt{2}\sin(3\pi/16)$ but its shape is kept constant.

In Fig.4(a) we show the dependency on the parameter θ by plotting several profiles of $|\psi_G(x,t)|^2$ with $\Omega = 1$ and different values of θ. For all gray solitons, the dip minimum always occurs at the dip center with a value of $|\psi_G(x_0,t)|^2 = \Omega\sin^2(\theta)$. Larger values of the phase θ correspond to the shallower center dips of the gray soliton. For the special case of $\theta = 0$ the dip minimum goes to zero as expected for dark solitons.

In Fig.4(b) we show several phase profiles $Arg(\psi_G(x,0))$ for the same values of θ as those in Fig.4(a). For a given value of θ, the spatial distribution of the phase of the gray soliton varies from $\pi - \theta$ at $x \to -\infty$ to θ at $x \to \infty$. It can also be seen that larger values of θ correspond to smoother spatial variation of the phase. For the special case of $\theta = 0$ we recover the dark soliton phase, an abrupt π shift at the dip center.

In the limit where $\theta = \pi/2$, the soliton has the same constant amplitude as the background and a constant phase of $\pi/2$, there is no dip and the solution recovers the background plane wave in Eq.(2) with a $\pi/2$ phase shift.

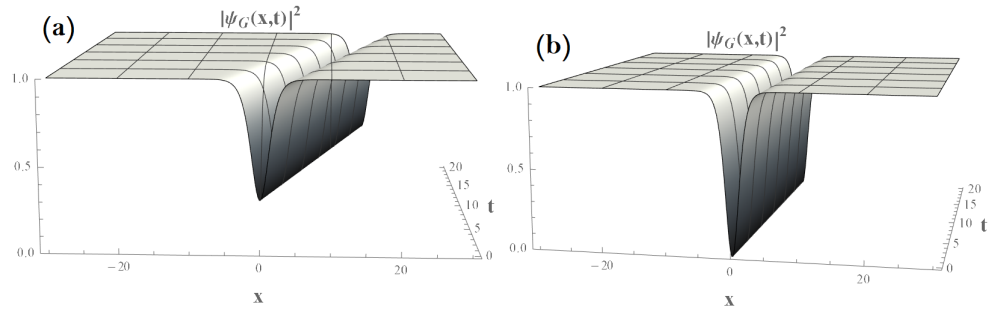

Figure 3: Spatio-temporal evolution of the amplitude of a **(a)** gray soliton with $\theta = 3\pi/16$ a **(b)** dark soliton (with $\theta = 0$). In both cases $\Omega = 1$. The gray soliton has a velocity of $v = \sqrt{2}\sin(3\pi/16)$ and it reaches its minimum of $\sin^2(3\pi/16)$ at its dip center while the dark soliton is stationary and reaches its minimum of zero also at its dip center.

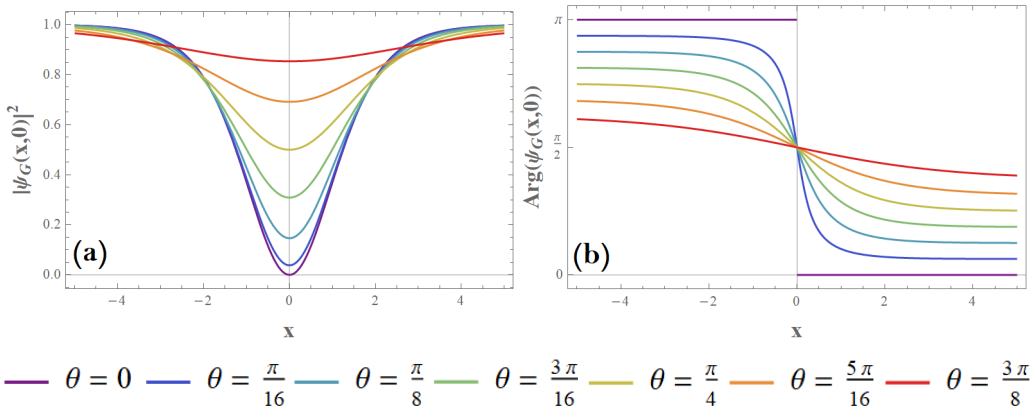

Figure 4: Spatial profiles of the **(a)** amplitude and the **(b)** phase of various gray solitons calculated with different values of θ (depicted in the legend).

4. Breather Soliton

4.1. Akhmediev Breather Solution

In this section we derive analytically the solution of the Akhmediev breather and show that is possible to obtain two other solutions, the Kuznetsov-Ma breather and the Peregrine soliton, solely by changing the interval of a certain parameter. As usual, we make an initial ansatz and show that under certain boundary condition and educated guesses and restrains one can obtain the desire solution.

Contrarily to what we did for the dark and gray soliton, this breather solution can only be formed within a self-focusing medium with non-zero unstable background. Because of this, we will be deriving the breather solution instead from the NLSE with $\sigma = +1$,

$$i\frac{\partial\psi}{\partial t} + \frac{\partial^2\psi}{\partial x^2} + |\psi(x,t)|^2\psi(x,t) = 0. \tag{44}$$

We start by making the ansatz by presupposing that only the real part of the amplitude, $Q(x,t)$, depends both on time and on the propagation coordinate, while the imaginary part of the amplitude, $\delta(t)$, and the phase, $\phi(t)$, depend upon time only

$$\psi(x,t) = [Q(x,t) + i\delta(t)]\exp[i\varphi(t)]. \tag{45}$$

Substituting this ansatz into Eq.(44) and separating the real and imaginary parts we obtain a system of two ordinary differential equations

$$-\varphi_t Q - \delta_t + Q_{xx} + Q^3 + \delta^2 Q = 0, \tag{46}$$

$$-\varphi_t\delta + Q_t + Q^2\delta + \delta^3 = 0. \tag{47}$$

To obtain the first integral of Eq.(46) we multiply it by $2Q_{xx}$ and integrate in the spatial coordinate on both sides, obtaining

$$-\varphi_t Q^2 - 2\delta_t Q + (Q_x)^2 + \frac{1}{2}Q^4 + \delta^2 Q^2 = h(t). \tag{48}$$

Note that the integration parameter $h(t)$ is not a constant - it depends on time because we integrated only on the spatial coordinate while $Q(x,t)$ and $\delta(t)$ are time-dependent.

We rewrite Eq.(48) in order to express explicitly the spatial derivative,

$$Q_x = \pm\sqrt{h + \varphi_t Q^2 + 2\delta_t Q - \frac{1}{2}Q^4 - \delta^2 Q^2}. \tag{49}$$

Similarly, we rewrite Eq.(47) to express explicitly the time derivative,

$$Q_t = \varphi_t \delta - Q^2\delta - \delta^3. \tag{50}$$

For the system of equations explicit in Eq.(46) and Eq.(47) to be compatible, the relation $Q_{xt} = Q_{tx}$ should be hold. On one hand, if we differentiate Eq.(49) with respect to time,

$$Q_{xt} = \pm\frac{h_t + \varphi_{tt}Q^2 + 2\varphi_t Q Q_t + 2\delta_{tt}Q + 2\delta_t Q_t - 2Q^3 Q_t - 2\delta\delta_t Q^2 - 2\delta^2 Q Q_t}{2\sqrt{h + \varphi_t Q^2 + 2\delta_t Q - \frac{1}{2}Q^4 - \delta^2 Q^2}}, \tag{51}$$

and substitute Q_t from Eq.(50) into the above equation, we obtain

$$Q_{xt} = \pm\frac{h_t + \varphi_{tt}Q^2 + 2\delta_{tt}Q - 2\delta\delta_t Q^2 + 2[\varphi_t Q + \delta_t - Q^3 - \delta^2 Q][\varphi_t\delta - Q^2\delta - \delta^3]}{2\sqrt{h + \varphi_t Q^2 + 2\delta_t Q - \frac{1}{2}Q^4 - \delta^2 Q^2}}. \tag{52}$$

One the other hand, differentiating Eq.(50) with respect to the space coordinate and substituting Q_x from Eq.(49) we obtain

$$Q_{tx} = -2\delta Q Q_x = \mp 2\delta Q\sqrt{h + \varphi_t Q^2 + 2\delta_t Q - \frac{1}{2}Q^4 - \delta^2 Q^2}. \tag{53}$$

Finally, matching the results from Eq.(52) and Eq.(53) we get

$$Q^2[\varphi_{tt} + 4\delta\delta_t] + 2Q[\delta_{tt} + \varphi_t^2\delta - \delta^3 - \delta^3\varphi_t - \delta^5 + 2\delta h] + [h_t + 2\delta_t\varphi_t\delta - 2\delta_t\delta^3) = 0. \tag{54}$$

Equating the terms in front of different powers of Q to zero, we obtain a system of three equations

$$h_t + 2\delta_t \left[\varphi_t \delta - \delta^3\right] = 0, \tag{55}$$

$$\delta_{tt} + \delta \left[\varphi_t - \delta^2\right]^2 = -2\delta h, \tag{56}$$

$$\varphi_{tt} = -4\delta\delta_t. \tag{57}$$

To solve this system of equation we start by integrating Eq.(57) with respect to time. Since all functions depend only on time the integration parameter will be effectively constant, this is

$$\varphi_t = -2\delta^2 + W. \tag{58}$$

Substituting this expression of φ_t in Eq.(55) and integrating it, we have

$$h + W\delta^2 - \frac{3}{2}\delta^4 = H. \tag{59}$$

From this, we obtained another constant parameter, the parameter H. With this results, we can substitute both φ_t from Eq.(58) and $h(t)$ from Eq.(59) into Eq.(56) to obtain

$$\delta_{tt} + \delta \left[W - 3\delta^2\right]^2 = -2\delta \left[H - W\delta^2 + \frac{3}{2}\delta^4\right]. \tag{60}$$

After multiplying the above equation by $2\delta_t$ and integrating the result, we introduce a new constant parameter D as

$$(\delta_t)^2 + \delta^2 \left[W^2 + 2H\right] - 4W\delta^4 + 4\delta^6 = D. \tag{61}$$

Since all powers of δ are even, it is convenient to make the substitution $z(t) = \delta^2(t)$. Noting that $(\delta_t)^2 = (z_t)^2/4z$ we rewrite Eq.(61) as

$$(z_t)^2 = -16z^4 + 16Wz^3 - 4[W^2 + 2H]z^2 + 4Dz. \tag{62}$$

Thus, we started with three real functions to determine $Q(x,t)$, $\delta(t)$ and $\varphi(t)$ and now we have three constant parameters (W, H and D) whom dictate the class of solutions [except for shifts with respect to both variables and rotations in the complex plane through a constant angle, as we saw in Eq.(35)]. Once we solve Eq.(62) and get the solution of $z(t) = \delta^2(t)$ we

shall backtrack to Eq.(59) to obtain $h(t)$. Then, with $h(t)$ known, we can go further back to Eq.(48) to obtain $Q(x,t)$. Up to this point we also have all the information to obtain $\varphi(t)$ from Eq.(58).

From this point on we consider the situation where the constants W, H and D are not independent but instead are parametrized by a constant a like

$$W = 4a - 1, \tag{63}$$
$$H = 4a - 1/2, \tag{64}$$
$$D = 16a^2. \tag{65}$$

Later, it will be seen that such choice will allow us to find the solution in the form of a breather (other choices of the constants W,H,D imposes another type of solutions). Substituting these expression into Eq.(62) allows one to rewrite this equation in a much simpler form,

$$\begin{aligned}(z_t)^2 &= -16z\left\{z^3 - (4a+1)z^2 + 4z\left[a^2 + a\right] - 4a^2\right\} \\ &= -16z(z-2a)^2(z-1).\end{aligned} \tag{66}$$

Because $\delta(t)$ is a real function, $z(t) = \delta^2(t)$ and $(z_t)^2$ is a positive value, for the self-consistence of the above equation, we need to require the right-hand side to be positive. The term $(z-2a)^2$ is always positive thus the condition $-z(z-1) > 0$ imposes positiveness of the right-hand side of Eq.(66). This implies that z is constrained to $0 < z < 1$. In order to solve Eq.(66) we introduce a new real function $f(t)$ and make the ansatz

$$z = \frac{2a\left[f^2 - 1\right]}{f^2 - 2a}. \tag{67}$$

Substituting this ansatz in Eq.(66) we obtain a rather simpler differential equation for $f(t)$ as

$$(f_t)^2 = -8a(2a-1)(f^2-1), \tag{68}$$

of solution

$$f(t) = \cosh(\alpha t), \tag{69}$$

where $\alpha = \sqrt{8a(1-2a)}$.

Because we defined $f(t)$ as a real function we need the right-hand side of Eq.(68) to be positive. We have three possible regimes:
1) $a < 0$ and $f > 1$; **2)** $a > 1/2$ and $f < 1$; **3)** $0 < a < 1/2$ and $f > 1$;
We will disregard regime **1)** because the negativeness of a implies the solution $f(t) = \cos\Big(\sqrt{8a(2a-1)}\ t\Big) < 1$ which is in contradiction with itself. Thus, it is only of our interest the cases **2)** and **3)** since they correspond respectively to the regime where the Akhmediev breather and Kuznetsov-Ma breather form. We will see that the remaining Peregrine soliton exists in the limit between this two regimes. From now on we follow the case **2)** where $a < 1/2$. Substituting the solution in Eq.(69) into Eq.(67) we rewrite $z(t)$ as

$$z = \frac{2a\sinh^2(\alpha t)}{\cosh^2(\alpha t) - 2a}. \tag{70}$$

As it was mentioned above, in order to obtain $Q(x,t)$ we need to backtrack to Eq.(48) and substitute the function $\varphi_t(t)$ from Eq.(58), $\delta(t) = \sqrt{z(t)}$ from Eq.(70), and $h(t)$ from Eq.(59), along with the parameters W and H from Eq.(63) and Eq.(64) respectively. We then obtain

$$\begin{aligned}(Q_x)^2 &= \varphi_t Q^2 + 2\delta_t Q - \frac{1}{2}Q^4 - \delta^2 Q^2 + h \\ &= (4a + 1 - 3z)Q^2 + 4Q\sqrt{(z-2a)^2(1-z)} - \frac{1}{2}Q^4 \\ &+ 4a - \frac{1}{2} - (4a+1)z + \frac{3}{2}z^2. \end{aligned} \tag{71}$$

This equation can be rewritten as

$$Q_x^2 = -\frac{1}{2}(Q - Q_3)^2(Q - Q_1)(Q - Q_2), \tag{72}$$

where

$$Q_1 = \sqrt{1-z} + 2\sqrt{2a-z}, \tag{73}$$
$$Q_2 = \sqrt{1-z} - 2\sqrt{2a-z}, \tag{74}$$
$$Q_3 = -\sqrt{1-z}. \tag{75}$$

Since we are following the case where $a < 1/2$, we have from Eq.(70) that $0 < z < 2a < 1$ and so, $Q_3 < 0$, $Q_2 - Q_3 > 0$ and $Q_1 - Q_2 > 0$ such that $Q_1 > Q_2 > Q_3$.

Analogous to what has been done for $z(t)$ in Eq.(67), we make the ansatz

$$Q = \frac{Q_1(Q_2 - Q_3) + Q_3(Q_1 - Q_2)g^2(x)}{(Q_2 - Q_3) + (Q_1 - Q_2)g^2(x)} \tag{76}$$

and substitute it into Eq.(72) to get a much simpler differential equation in terms of a new real spacial function $g(x)$,

$$\begin{aligned} 4(g_x)^2 &= \frac{1}{2}(Q_1 - Q_3)(Q_2 - Q_3)\left[1 - g^2\right] \\ &= 2(1 - 2a)\left[1 - g^2\right], \end{aligned} \tag{77}$$

whose solution can be expressed as

$$g(x) = \sin\left(\frac{\beta x}{2}\right) \tag{78}$$

where $\beta = \sqrt{2(1 - 2a)}$.

Since in our case $a < 1/2$ and $g < 1$ [last fact follows from the properties of the *sin* in Eq.(78)], the right-hand side of Eq.(77) is positive, which proofs self-consistency of this equation and its solution.

Substituting Eq.(73), Eq.(74), Eq.(75) and Eq.(78) in Eq.(76) we obtain an expression for Q in the form

$$Q = \frac{(1 - z) - 2(2a - z) + \sqrt{1 - z}\sqrt{2a - z}\cos(\beta x)}{\sqrt{1 - z} - \sqrt{2a - z}\cos(\beta x)}. \tag{79}$$

Now, if we substitute the following expressions taken from Eq.(70),

$$\sqrt{1 - z} = \frac{\beta}{\sqrt{2}}\frac{\cosh(\alpha t)}{\sqrt{\cosh^2(\alpha t) - 2a}}, \tag{80}$$

$$\sqrt{2a - z} = \frac{\sqrt{a}\beta}{\sqrt{\cosh^2(\alpha t) - 2a}}, \tag{81}$$

we can write Q's final expression as

$$Q = \frac{\beta}{\sqrt{2}\sqrt{\cosh^2(\alpha t) - 2a}}\frac{\cosh^2(\alpha t) - 4a + \sqrt{2a}\cosh(\alpha t)\cos(\beta x)}{\cosh(\alpha t) - \sqrt{2a}\cos(\beta x)}. \tag{82}$$

With $Q(x,t)$ and $\delta(t)$ known, it is now possible to obtain the remaining function from our initial ansatz, the phase $\varphi(t)$. Integrating Eq.(58) we obtain

$$\begin{aligned}\varphi(t) &= (4a+1)t - 2\int_0^t z(t')dt' \\ &= (4a+1)t - 4a\int_0^t \frac{\sinh^2(\alpha t')}{\cosh^2(\alpha t') - 2a}dt'.\end{aligned} \tag{83}$$

This expression can be rewritten in terms of $\tanh(\alpha t)$ as

$$\begin{aligned}\varphi(t) &= (4a+1)t + \frac{4a}{1-2a}\int_0^t \left[\frac{1}{1+\frac{2a}{1-2a}\tanh^2(\alpha t')}\frac{\tanh^2(\alpha t')}{\tanh^2(\alpha t') - 1}\right][1-\tanh^2(\alpha t')]dt' \\ &= (4a+1)t + 4a\int_0^t \left[\frac{1}{1+\frac{2a}{1-2a}\tanh^2(\alpha t')} + \frac{1}{\tanh^2(\alpha t') - 1}\right][1-\tanh^2(\alpha t')]dt'.\end{aligned} \tag{84}$$

Here we expressed the first term inside the squared brackets as a sum, this way the second integral greatly simplifies. We obtain

$$\varphi(t) = (4a+1)t + \frac{4a}{\alpha}\int_0^t \frac{1}{1+\frac{2a}{1-2a}\tanh^2(\alpha t')}d\tanh(\alpha t') - 4a\int_0^t dt'. \tag{85}$$

After the following substitution,

$$\varphi(t) = t + \frac{4a}{\sqrt{8a(1-2a)}}\sqrt{\frac{1-2a}{2a}}\int_0^t \frac{1}{1+\frac{2a}{1-2a}\tanh^2(\alpha t')}d\left[\sqrt{\frac{2a}{1-2a}}\tanh(\alpha t')\right], \tag{86}$$

and integration, the expression for the phase $\varphi(t)$ can be written in its final form as

$$\varphi(t) = t + \arctan\left(\sqrt{\frac{2a}{1-2a}}\tanh(\alpha t)\right). \tag{87}$$

In order to substitute in the original ansatz in Eq.(45), we represent the phase term explicitly as

$$e^{i\varphi(t)} = e^{it}\left[\cos\left\{\arctan\left(\sqrt{\frac{2a}{2a-1}}\tan(\alpha t)\right)\right\} + i\sin\left\{\arctan\left(\sqrt{\frac{2a}{2a-1}}\tan(\alpha t)\right)\right\}\right]. \tag{88}$$

Using the trigonometric relations $\frac{1}{\cos^2(x)} = 1 + \tan^2(x)$ and $\sin^2(x) = \frac{\tan^2(x)}{1+\tan^2(x)}$, the phase term in Eq.(88) can be rewritten as

$$e^{i\varphi(t)} = e^{it}\frac{1 + i\sqrt{\frac{2a}{2a-1}}\tan(\alpha t)}{\sqrt{1 + \frac{2a}{2a-1}\tan^2(\alpha t)}}. \tag{89}$$

We can now substitute $Q(x,t)$ from Eq.(82), $\delta(t) = \sqrt{z(t)}$ from Eq.(70) and $e^{i\varphi(t)}$ from Eq.(89) into Eq.(45) to obtain the solution

$$\psi(x,t) = e^{it}\frac{1 + i\sqrt{\frac{2a}{1-2a}}\tanh(\alpha t)}{\sqrt{1 + \frac{2a}{1-2a}\tanh^2(\alpha t)}}\left[i\frac{\sqrt{2a}\sinh(\alpha t)}{\sqrt{\cosh^2(\alpha t) - 2a}} + \right.$$
$$\left. + \frac{\beta}{\sqrt{2}\sqrt{\cosh^2(\alpha t) - 2a}}\frac{\cosh^2(\alpha t) - 4a + \sqrt{2a}\cosh(\alpha t)\cos(\beta x)}{\cosh(\alpha t) - \sqrt{2a}\cos(\beta x)}\right]. \tag{90}$$

With the aim of simplifying terms, it's useful to note that the square-rotted term in the denominator of the exponential can be expressed as

$$1 + \frac{2a}{1-2a}\tanh^2(\alpha t) = \frac{1}{1-2a}\frac{\cosh^2(\alpha t) - 2a}{\cosh^2(\alpha t)}. \tag{91}$$

This way, the term $\sqrt{\cosh^2(\alpha t) - 2a}$ appears in denominator twice and we can get rid of the squared root. Thus, Eq.(88) can be simplified as

$$\begin{aligned}\psi(x,t) = \frac{e^{it}}{\sqrt{2}} \frac{1}{\cosh(\alpha t) - \sqrt{2a}\cos(\beta x)} \frac{\sqrt{1-2a}\cosh(\alpha t) + i\sqrt{2a}\sinh(\alpha t)}{\cosh^2(\alpha t) - 2a} \times \\ \times \left[\beta \left\{\cosh^2(\alpha t) - 4a + \sqrt{2a}\cosh(\alpha t)\cos(\beta x)\right\} + \right. \\ \left. + \, i2\sqrt{a}\sinh(\alpha t)\left\{\cosh(\alpha t) - \sqrt{2a}\cos(\beta x)\right\}\right]. \end{aligned} \tag{92}$$

After expanding terms the above expression will have the form

$$\begin{aligned}\psi(x,t) = \frac{e^{it}}{\cosh(\alpha t) - \sqrt{2a}\cos(\beta x)} \frac{1}{\cosh^2(\alpha t) - 2a} \times \\ \times \left[(1-2a)\left\{\cosh^3(\alpha t) - 4a\cosh(\alpha t) + \sqrt{2a}\cosh^2(\alpha t)\cos(\beta x)\right\} - \right. \\ - 2a\sinh^2(\alpha t)\left\{\cosh(\alpha t) - \sqrt{2a}\cos(\beta x)\right\} + \\ + i\left\{\sqrt{2a}\sqrt{1-2a}\cosh(\alpha t)\sinh(\alpha t)\left\{\cosh(\alpha t) - \sqrt{2a}\cos(\beta x)\right\} + \right. \\ \left.\left. + \, \sqrt{a}\sinh(\alpha t)\,\beta\left\{\cosh^2(\alpha t) - 4a + \sqrt{2a}\cosh(\alpha t)\cos(\beta x)\right\}\right\}\right]. \end{aligned} \tag{93}$$

Notice that the term $\sqrt{a}\sinh(\alpha t)\beta\sqrt{2a}\cosh(\alpha t)\cos(\beta x)$ at the end of the two last terms cancel out. Rearranging common terms and cancelling out others doing some algebraic manipulation the expression greatly simplifies to

$$\begin{aligned}\psi(x,t) = \frac{e^{it}}{\cosh(\alpha t) - \sqrt{2a}\cos(\beta x)} \times \\ \times \left[(1-4a)\cosh(\alpha t) + \sqrt{2a}\cos(\beta x) + i\alpha\sinh(\alpha t)\right]. \end{aligned} \tag{94}$$

Using the definition under Eq.(78) that $\beta = \sqrt{2(1-2a)}$ we have that $(1-4a)\cosh(\alpha t) = \beta^2\cosh(\alpha t) - \cosh(\alpha t)$. Note that, this way, there is a common term with the denominator (except for an irrelevant minus sign that represents a global phase) and for last, we obtain the final expression for the Akhmediev breather solution as

$$\psi_A(x,t) = \left[1 + \frac{\beta^2 \cosh(\alpha t) + i\alpha \sinh(\alpha t)}{\sqrt{2a}\cos(\beta x) - \cosh(\alpha t)}\right] e^{it}, \tag{95}$$

where $0 < a < 1/2$, $\beta = \sqrt{2(1-2a)}$ and $\alpha = 2\sqrt{a}\beta$.

To visually represent the property of this type of solutions we plotted in Fig.5 the amplitude of two Akhmediev breathers as a function of time and propagation distance. The first [see Fig.5(a)] is characterized by the parameter $a = 0.25$ and the second one [shown in Fig.5(b)] by $a = 0.00001$. As it can be seen, the key point of this type of waves is that they are localized in time but oscillate in space. The function reaches its maximum at a certain time $t_0 = 0$ (in this case $t_0 = 0$) as an oscillating pattern in space and then quickly fades away to the amplitude of the unstable plane wave background.

Note that the amplitude and time scales are immensely different. While the breather in Fig.5(a) exists only in a range of $\approx 10s$ with a maximum amplitude of $\psi_A(0,0) \approx 5.8$, the breather in Fig.5(b) exists during $\approx 1000s$ with a maximum amplitude of $\psi_A(0,0) \approx 1.018$ being just slightly above the background. For bigger values of the parameter a the maximum amplitude increases by

$$|\psi_{A_{max}}(a)|^2 = \left(1 + \frac{2(1-2a)}{\sqrt{2a}-1}\right)^2. \tag{96}$$

For smaller values of the parameter a the localization in time starts to "spread" and at the limit where $a \to 0$ it extends over all time with an amplitude equal to the non-zero background i.e., only remains the plane wave background.

However, the propagation distance scale is the same for the two figures. The breather at Fig.5(a) does approximately three full oscillations while the one at Fig.5(b) already did approximately five full oscilattion. The frequency of oscillation in space for a Akhmediev breather depends on a as

$$\omega_A(a) = \beta = \sqrt{2(1-2a)} \tag{97}$$

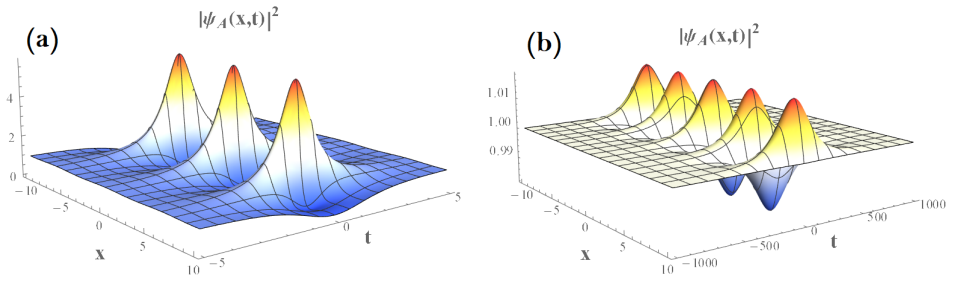

Figure 5: Spatio-temporal evolution of the squared amplitude of the Akhmediev breather with **(a)** $a = 0.25$ and **(b)** $a = 0.00001$.

4.2. Kuznetsov-Ma Breather Solution

To obtain the Kuznetsov-Ma breather solution, as we mentioned above when we made explicit the three possible regimes for the solutions of Eq.(68) and Eq.(77), we need to evaluate the Akhmediev breather solution in the regime where the parameter is in the interval $a > 1/2$ instead of $0 < a < 1/2$.

We start by identifying that in this new interval $\beta = \sqrt{2(1-2a)}$ is a purely imaginary value instead of a real one. Thereby, we define a new constant β' such that $\beta = i\beta'$ and, because α depends on β, we also define α' such that $\alpha = i\alpha'$. It's easy to see that expanding the trigonometric functions into their exponential forms and substituting for this new constants we obtain the following relations with the hyperbolic functions:
$\cosh(\alpha t) = \cos(\alpha' t)$, $\sinh(\alpha) = i\sinh(\alpha' t)$ and $\cos(\beta x) = \cosh(\beta' x)$. Substituting this expressions into Eq.(95) we obtain the Kuznetsov-Ma breather solution as

$$\psi_{KM}(x,t) = \left[1 - \frac{(\beta')^2\cos(\alpha' t) + i\alpha'\sin(\alpha' t)}{\sqrt{2a}\cosh(\beta' x) - \cos(\alpha' t)}\right] e^{it}, \tag{98}$$

where $a > 1/2$, $\beta' = \sqrt{2(2a-1)}$ and $\alpha = 2\sqrt{a}\beta'$.

Again, to visually represent the properties of this type of solutions we plotted in Fig.6 the squared amplitude of two Kuznetsov-Ma breathers as a function of time and propagation distance. The first breather [depicted in Fig.6(a)] is characterized by the parameter $a = 0.8$ and the second one [shown in Fig.6(b)] by $a = 2$. Contrarily to what we saw in the Akhmediev breather solution, this type of waves are localized in space but oscillate in time. Elsewhere expect in the vicinity of some value of x_0 (in this case $x_0 = 0$) the function amplitude is close to that of the unstable plane wave

background. At the same time, the amplitude at $x = x_0$ oscillates up and down like a snorkeller swimming up and down gasping for air, hence the term "breather".

Note that the amplitude scales are different between the two figures. While the first breather [in Fig.6(a)] reaches a maximum of amplitude of $|\psi_{KM}(0,0)|^2 \approx 12.46$, the second one [in Fig.6(b)] reaches a maximum of $|\psi_{KM}(0,0)|^2 \approx 25$. For larger values of the parameter a the solution achieves increasingly higher amplitudes

$$|\psi_{KM_{max}}|^2 = \left(1 - \frac{2(2a-1)}{\sqrt{2a}-1}\right)^2 . \tag{99}$$

However, both the time scale t and propagation distance scale x are the same for the two figures which means that breather at Fig.6(b) oscillates a lot faster than the one at Fig.6(a). This happens because the frequency of oscillation in time for a Kuznetsov-Ma breather depends on a as

$$\omega_{KM}(a) = \beta' = \sqrt{2(2a-1)} \tag{100}$$

As it can be see from the two examples, the bigger the value of the parameter a the more localized in space the wave is, although this difference is not as prominent as the differences between two Akhmediev breather.

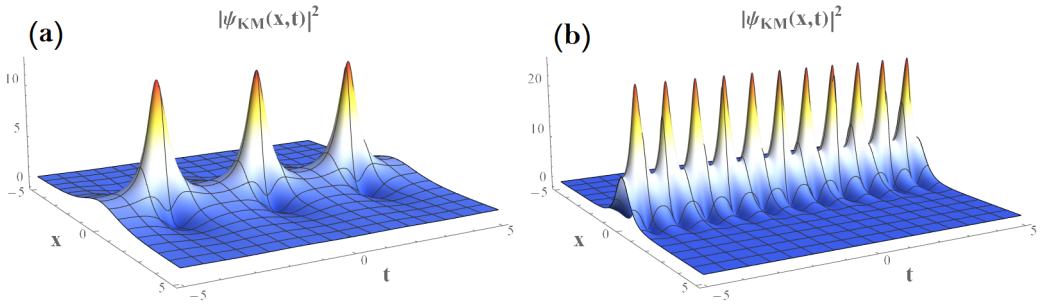

Figure 6: Spatio-temporal evolution of the squared amplitude solution of the Kuznetsov-Ma breather with **(a)** $a = 0.8$ and **(b)** $a = 2$

4.3. Peregrine Soliton Solution

For last, the Peregrine soliton solution is obtained at the intermediate regime in the limit when $a \to 1/2$. It's important to note that the function is not defined at $a = 1/2$ because if we substitute directly in the Akhmediev breather solution in Eq.(95) we end up with an indeterminate form $0/0$. This way, we resorted to Taylor expansion. We start by noting that as $a \to 1/2$ we get $\beta \to 0$ and consequently $\alpha \to 0$, and so

$$\alpha = 2\sqrt{a}\beta = 2\sqrt{\frac{1}{2} - \frac{\beta^2}{4}}\beta = \beta\sqrt{2 - \beta^2} \approx \sqrt{2}\beta. \tag{101}$$

The factor $\sqrt{2a}$ is expressed as

$$\sqrt{2a} = \sqrt{1 - \frac{\beta^2}{2}} \approx 1 - \frac{\beta^2}{4}, \tag{102}$$

and the trigonometric and hyperbolic functions as

$$\begin{aligned} \cos(\beta x) &\approx 1 - \frac{(\beta x)^2}{2}, \\ \sinh(\alpha t) &\approx \alpha t \approx \sqrt{2}\beta t, \\ \cosh(\alpha t) &\approx 1 + \frac{(\alpha t)^2}{2} \approx 1 + (\beta t)^2. \end{aligned} \tag{103}$$

Substituting this expansions back in Eq.(95) we obtain

$$\begin{aligned} \psi(x,t) &= e^{it}\left[1 + \frac{(\beta)^2\left\{1 + (\beta t)^2\right\} + i\sqrt{2}\beta\sqrt{2}\beta t}{\left\{1 - \frac{(\beta)^2}{4}\right\}\left\{1 - \frac{(\beta x)^2}{2}\right\} - 1 - (\beta t)^2}\right], \\ &= e^{it}\left[1 + \frac{(\beta)^2 + 2i\,(\beta)^2\, t}{1 - \frac{(\beta)^2}{4} - \frac{(\beta x)^2}{2} - 1 - (\beta t)^2}\right], \end{aligned} \tag{104}$$

which leads directly to the final expression of the Peregrine soliton

$$\psi_P(x,t) = \left[1 - 4\frac{1 + 2it}{1 + 2x^2 + 4t^2}\right] e^{it} \tag{105}$$

In Fig.7 we plotted the squared amplitude of this solution. As it can be seen, this soliton solution is localized in both time and space because it corresponds to the limiting case of infinite period of both the space-periodic Akhmediev breather and the time-periodic Kuznetsov-Ma breather. This type of waves starts as a weak oscillation on a non-zero continuous background but suddenly, it rapidly increases its amplitude forming a sharp peak who quickly fades away unnoticed. At maximum amplitude, this solution has an amplitude that is $9\times$ larger than the non-zero continuous background, in this case $|\psi_P(0,0)|^2 = 9$.

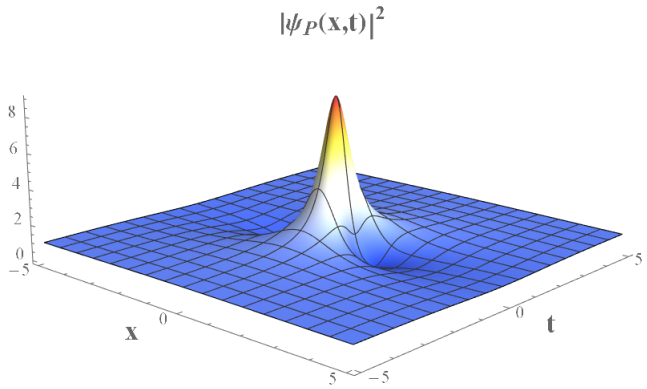

Figure 7: Spatio-temporal evolution of the amplitude solution of the Peregrine soliton.

5. Conclusion

To conclude, we have obtained analytically two different sets of soliton solutions of the NLSE namely the dark solitons and the breathers.

Firstly, we considered the stability of a plane wave background with respect to small perturbations (modulational instability) and demonstrated that the plane wave solution is stable in the self-defocusing case ($\sigma < 0$) and unstable in the self-focusing case ($\sigma > 0$). This analysis was critical because the required solutions can be formed only under certain conditions: dark solitons only exists in a self-defocusing medium with a constant amplitude stable background while the breathers only exists in a self-focusing medium with a non-zero unstable background.

Secondly, we have analytically obtained the family of NLSE solutions in the form of a gray soliton - non-stationary dips that propagate with constant velocity, maintaining their shape along its propagation, and whose minimum

amplitude, velocity and frequency are determined by the amplitude ρ of the constant amplitude background. We have shown that the special solution of the dark soliton (whose minimal amplitude attains zero) is the limiting case of a gray soliton when the single parameter θ is zero. The dark soliton is a stationary (non-moving) dip with a characteristic tanh profile and an abrupt π shift at the dip's center.

Thirdly, we have analytically obtained the family of breather solutions in the form of the Ahkmediev breather, the Kuznetsov-Ma breather and the Peregrine soliton, and demonstrated that these solutions are related to each other depending upon the value of the parameter a ($0 < a < 1/2$, $a \to 1/2$, and $a > 1/2$ for the Akhmediev breather, the Kuznetsov-Ma breather and the Peregrine soliton, respectively). We have also demonstrated that the Akhmediev breather is localized in time but oscillates in space, the Kuznetsov-Ma breather is localized in space but oscillates in time, and the Peregrine soliton is localized both in time and space (as it can be considered an intermediate case between the Kuznetsov-Ma and Akhmediev breathers).

References

[1] L. F. Mollenauer and J. P. Gordon, *Solitons in optical fibers: fundamentals and applications*. Amsterdam ; Boston: Elsevier/Academic Press, 2006. OCLC: ocm62290481.

[2] D. Kachulin, A. Dyachenko, and V. Zakharov, "Soliton Turbulence in Approximate and Exact Models for Deep Water Waves," *Fluids*, vol. 5, p. 67, May 2020.

[3] Y. Kodama, "KP solitons in shallow water," *Journal of Physics A: Mathematical and Theoretical*, vol. 43, p. 434004, Oct. 2010.

[4] F. K. ABDULLAEV, A. Gammal, A. M. Kamchatnov, and L. Tomio, "DYNAMICS OF BRIGHT MATTER WAVE SOLITONS IN A BOSE–EINSTEIN CONDENSATE," *International Journal of Modern Physics B*, vol. 19, pp. 3415–3473, Sept. 2005.

[5] M. L. Nesterov, J. Bravo-Abad, A. Y. Nikitin, F. J. García-Vidal, and L. Martin-Moreno, "Graphene supports the propagation of subwavelength optical solitons: Optical solitons in graphene," *Laser & Photonics Reviews*, vol. 7, pp. L7–L11, Mar. 2013.

[6] W. Walasik and G. Renversez, "Plasmon-soliton waves in planar slot waveguides. I. Modeling," *Physical Review A*, vol. 93, p. 013825, Jan. 2016.

[7] A. Hasegawa and F. Tappert, "Transmission of stationary nonlinear optical pulses in dispersive dielectric fibers. I. Anomalous dispersion," *Applied Physics Letters*, vol. 23, pp. 142–144, Aug. 1973.

[8] A. D. Boardman, P. Bontemps, T. Koutoupes, and K. Xie, "Temporal and Spatial Solitons: An Overview," in *Beam Shaping and Control with Nonlinear Optics* (F. Kajzar and R. Reinisch, eds.), vol. 369, pp. 183–228, Boston: Kluwer Academic Publishers, 2002. Series Title: NATO Science Series: B:.

[9] B. A. Malomed, D. Mihalache, F. Wise, and L. Torner, "Spatiotemporal optical solitons," *Journal of Optics B: Quantum and Semiclassical Optics*, vol. 7, pp. R53–R72, May 2005.

[10] C. M. de Sterke, B. J. Eggleton, and J. E. Sipe, "Bragg Solitons: Theory and Experiments," in *Spatial Solitons* (W. T. Rhodes, S. Trillo, and W. Torruellas, eds.), vol. 82, pp. 169–209, Berlin, Heidelberg: Springer Berlin Heidelberg, 2001. Series Title: Springer Series in Optical Sciences.

[11] Y. V. Bludov, V. V. Konotop, and M. Salerno, "Dynamical localization of gap-solitons by time periodic forces," *EPL (Europhysics Letters)*, vol. 87, p. 20004, July 2009.

[12] D. N. Christodoulides and R. I. Joseph, "Discrete self-focusing in nonlinear arrays of coupled waveguides," *Optics Letters*, vol. 13, p. 794, Sept. 1988.

[13] N. K. Efremidis, S. Sears, D. N. Christodoulides, J. W. Fleischer, and M. Segev, "Discrete solitons in photorefractive optically induced photonic lattices," *Physical Review E*, vol. 66, p. 046602, Oct. 2002.

[14] Y. S. Kivshar and G. P. Agrawal, *Optical solitons: from fibers to photonic crystals*. Amsterdam ; Boston: Academic Press, 2003.

[15] P. S. Lomdahl, "What Is a Soliton?," *LOS ALAMOS SCIENCE Spring*, 1984.

[16] L. Moraru, "Solitons - A Bridge between Mathematics and Physics," *JSM Math Stat*, vol. 1, no. 1, p. 1001, 2014.

[17] Y. S. Kivshar and X. Yang, "Dynamics of dark solitons," *Chaos, Solitons & Fractals*, vol. 4, pp. 1745–1758, Aug. 1994.

[18] D. N. Christodoulides and M. I. Carvalho, "Bright, dark, and gray spatial soliton states in photorefractive media," *Journal of the Optical Society of America B*, vol. 12, p. 1628, Sept. 1995.

[19] A. Chabchoub, O. Kimmoun, H. Branger, C. Kharif, N. Hoffmann, M. Onorato, and N. Akhmediev, "Gray solitons on the surface of water," *Physical Review E*, vol. 89, p. 011002, Jan. 2014.

[20] S. Burger, K. Bongs, S. Dettmer, W. Ertmer, K. Sengstock, A. Sanpera, G. V. Shlyapnikov, and M. Lewenstein, "Dark Solitons in Bose-Einstein Condensates," *Physical Review Letters*, vol. 83, pp. 5198–5201, Dec. 1999.

[21] L. Khaykovich, "Formation of a Matter-Wave Bright Soliton," *Science*, vol. 296, pp. 1290–1293, May 2002.

[22] F. K. Abdullaev and J. Garnier, "Bright Solitons in Bose-Einstein Condensates: Theory," in *Emergent Nonlinear Phenomena in Bose-Einstein Condensates* (P. G. Kevrekidis, D. J. Frantzeskakis, and R. Carretero-González, eds.), vol. 45, pp. 25–43, Berlin, Heidelberg: Springer Berlin Heidelberg, 2008. Series Title: Atomic, Optical, and Plasma Physics.

[23] R. H. Stolen, W. J. Tomlinson, and L. F. Mollenauer, "Observation of pulse restoration at the soliton period in optical fibers," *Optics Letters*, vol. 8, p. 186, Mar. 1983.

[24] E. A. Kuznetsov, "Solitons in Parametrically Unstable Plasma," *Sov. Phys. Dokl.*, pp. 507–508, 1977.

[25] Y.-C. Ma, "The Perturbed Plane-Wave Solutions of the Cubic Schrödinger Equation," *Studies in Applied Mathematics*, vol. 60, pp. 43–58, Feb. 1979.

[26] N. N. Akhmediev, V. M. Eleonskii, and N. E. Kulagin, "Exact first-order solutions of the nonlinear Schrodinger equation," *Theoretical and Mathematical Physics*, vol. 72, pp. 809–818, Aug. 1987.

[27] N. N. Akhmediev and V. I. Korneev, "Modulation instability and periodic solutions of the nonlinear Schrödinger equation," *Theoretical and Mathematical Physics*, vol. 69, pp. 1089–1093, Nov. 1986.

[28] D. H. Peregrine, "Water waves, nonlinear Schrödinger equations and their solutions," *The Journal of the Australian Mathematical Society. Series B. Applied Mathematics*, vol. 25, pp. 16–43, July 1983.

[29] L.-C. Zhao, L. Ling, and Z.-Y. Yang, "Mechanism of Kuznetsov-Ma breathers," *Physical Review E*, vol. 97, p. 022218, Feb. 2018.

[30] M. A. Alejo, L. Fanelli, and C. Muñoz, "Review on the Stability of the Peregrine and Related Breathers," *Frontiers in Physics*, vol. 8, p. 591995, Nov. 2020.

[31] N. Akhmediev, A. Ankiewicz, and M. Taki, "Waves that appear from nowhere and disappear without a trace," *Physics Letters A*, vol. 373, pp. 675–678, Feb. 2009.

[32] N. Akhmediev, "Waves that Appear From Nowhere: Complex Rogue Wave Structures and Their Elementary Particles," *Frontiers in Physics*, vol. 8, p. 612318, Jan. 2021.